

Rare earth oxides effects on both the threshold voltage and energy absorption capability of ZnO varistors

Mourad Houabes^{*}, Renaud Metz

Laboratoire Hydrazines et Procédés, UMR 5179 Lyon1-CNRS-ISOCHEM (Groupe SNPE), Université Claude Bernard Lyon1,
22 Avenue Gaston Berger, bâtiment Berthollet 69622 Villeurbanne Cedex, France

Received 13 October 2005; received in revised form 2 March 2006; accepted 6 April 2006

Available online 17 August 2006

Abstract

Rare earth oxides: Pr_6O_{11} , Y_2O_3 , La_2O_3 , Ce_2O_3 and Nd_2O_3 are added with contents of 0.01–0.5 wt.% to ZnO standard and antimony-rich varistor compositions. It is found that the rare earth oxide: REO, allows reaching large energy absorption capability value for the high threshold voltage ZnO-based varistors. A 30% maximum increase in threshold voltage is observed with the addition of 0.1 wt.% REO. However, degradation is accentuated with REO addition. Between 0 and 0.1 wt.% of REO the degradation remain still acceptable, but beyond 0.1% it becomes strong, up to 20% and energy absorption capability remains more than 100 J/cm^3 . It is practically constant whatever the REO percentage. Results from standard composition are exploited for the second composition by optimization of Sb_2O_3 and REO concentrations in order to control the growth of the ZnO grains while maintaining the energy absorption capability above 100 J/cm^3 . On the one hand, a high threshold voltage 300 V/mm ensured by antimony oxide, and on the other hand, a good capacity for absorption in energy 107 J/cm^3 ensured by the REO, whereas it had fallen to 52 J/cm^3 because of the great quantity of Sb_2O_3 . Satisfactory values of non-linearity coefficient (α) between 40 and 52 are obtained. These results are explained by the presence of extra-pyrochlore phase suggesting less bismuth oxide in the ceramics, especially at grain boundaries. Varistors present more active grains and hence a larger conduction section which account for large absorption capability.

© 2006 Elsevier Ltd and Techna Group S.r.l. All rights reserved.

Keywords: C. Electrical properties; E. Varistors; ZnO-based ceramics

1. Introduction

ZnO-based varistors are polycrystalline ceramics used to protect the electronic and electric components from transitory overvoltages [1]. Their main property is the high non-linearity of their characteristic current–voltage (I – V):

$$I = KV^\alpha \quad (1)$$

where K is a constant and α is the non-linearity coefficient.

Careful control of both processing parameters and the composition allows the use of ZnO varistors in many electrical and electronic at high and low voltage networks [1]. Moreover, the ceramics can draw current through them from several kilo amperes and handle energies up to 100 J/cm^3 [2,3].

Three significant parameters characterize the varistor: the non-linearity coefficient α , the threshold voltage V_s and the leakage current I_f . Satisfactory values of α ranging between 30 and 50 and I_f below 1 mA are obtained for ordinary ZnO varistors [4]. However, the values of V_s of about 100–200 V/mm for the average and high voltage lightning surge arrestors might be improved.

Commercial varistors are usually made by solid state of ZnO particles with doping agent oxides such as Bi_2O_3 , Sb_2O_3 , CoO , Mn_2O_3 and Cr_2O_3 , the mixed powder then being pressed and sintered at higher temperatures. The basic building block of the varistor microstructure consists of matrix of ZnO grains separated by grain boundaries providing p–n junction semiconductor characteristic [5]. During the sintering process, various metal oxide additives used in the composition get distributed in such a way that the final ZnO grain size after sintering is of the order of 15–20 μm surrounded by oxide phases (mainly $\text{Zn}_2\text{Bi}_3\text{Sb}_3\text{O}_{14}$ pyrochlore phase and $\text{Zn}_7\text{Sb}_2\text{O}_{12}$ spinel phase), grain boundaries and few pores. As the non-linear electrical behavior occurs at boundary of each semi-conducting

^{*} Corresponding author. Tel.: +33 4 72 44 83 27; fax: +33 4 72 43 12 91.

E-mail addresses: houabes@yahoo.fr (M. Houabes), metz@univ-lyon1.fr (R. Metz).

ZnO grain, the varistor can be defined as a multi-junction device composed of series and parallel connections of grain boundaries [6]. Thus, to achieve a given breakdown voltage, one can change the varistor thickness or one can vary the grain size to increase the number of barriers or grain boundaries, n . In either case, the macroscopic voltage between the electrodes is related to the microscopic voltage difference lying between two adjacent grains by the simple formula [2,4]:

$$V_s = \frac{3d}{D} \quad (2)$$

where D is the average size of ZnO grains, and d is the varistor thickness.

To increase the threshold voltage, it is necessary to decrease the average size of the ZnO grains [4]. Several works were interested in this objective [6–10], adding mainly oxides of antimony or lithium in the starting composition, and by decreasing the sintering temperature [4]. However, one is always confronted with the same dilemma: the highest the threshold voltage, the lowest is the energy absorption capability.

The rare earth oxides (REO) were used in the varistors technology to replace bismuth oxide [11,18] with the aim to study the non-linear I – V characteristics of doped zinc oxide ceramics. This gives rise to the increase of effective grain boundary area and ultimately enhances surge-absorption capability [11–18].

In this work, a new ceramic composition is proposed and consists in using rare earth oxides: Pr_6O_{11} , Y_2O_3 , La_2O_3 , Ce_2O_3 and Nd_2O_3 . Our goal is to study the REO effects on both the threshold voltage and the energy absorption capability of the ZnO varistors.

2. Experimental details

2.1. Samples preparation

The samples were prepared by the ceramics traditional method. Table 1 shows the standard chemical composition (SC) and the composition antimony-rich (CR). The oxide powders are weighed and mixed during 24 h with organic binder substances in earthenware jar with rollers and distilled water. The aqueous slurry obtained is dried at 200 °C during 10 h to produce granulates. The REO is then added in various quantities and a new dry milling of the powders is carried out during 10 h. After sieving appropriate fractions (150 μm) to extract dust and large agglomerated particles, the material is transferred to hydraulic pressing machines. The bodies are molded in discs of 30 mm in diameter, in quantities corresponding to 2 mm thickness. Batches of five samples for each composition are elaborated. The “green”

bodies are then sintered at 1200 °C during 1 h. The sintered pellets were polished and ohmic Pt–Ag contacts were realized. An annealing until 650 °C during half an hour ensures the good fixing of the electrodes. Then the bodies are coated on the side part by an epoxy resin. The samples are ready for the tests.

2.2. Electric tests

The I – V characteristics are measured, at low currents until 10 mA, under continuous voltage. A supply (Fug HCN 0–12.5 kV, 25 mA) outputs on the sample. The current I through the varistor is measured with an amperemeter (Keithley 619). The voltage V , between ceramic electrodes, is measured with a voltmeter (Racal Dana 6000) through a probe which divides the signal per 1000.

At the high current values, two shock wave generators are used, one of long duration (2 ms/0–500 A) and the other of short duration (4/10 μs /0–65 kA). The voltage and the current are visualized and measured on the screen of a numerical storage oscilloscope Tektronix 7633. To record a value of the current and the voltage, the average of the measurements made for five samples of the same batch is calculated.

2.3. Analyses of microstructure

Both the secondary electron mode and BE mode (back-scattered electrons) SEM/EDS photomicrostructures, were carried out by the use of a scanning electron microscope performed using JSM-6400 instrument. The crystallographic analysis was carried out by the use of X-ray diffraction method on sample polished surfaces.

2.4. Analyses of I – V characteristic

To analyze the results, it is determined from the I – V curves:

- the threshold voltage V_s (V/mm) which is given at a current density of 1 mA/cm²,
- the non-linearity coefficient:

$$\alpha = \frac{1}{\log(V_{10}/V_1)} \quad (3)$$

- where V_{10} and V_1 are the voltage values corresponding, respectively, to currents of 10 and 1 mA,
- degradation coefficient:

$$D = \frac{(V_{sb} - V_{sa})100}{V_{sb}} \quad (4)$$

Table 1
Chemical compositions: a standard chemical composition (SC) modified each time by one of the REO: Pr_6O_{11} , Y_2O_3 , La_2O_3 or Ce_2O_3 and composition antimony-rich (CR) modified only by Pr_6O_{11}

Composition	Oxide (mol.%)										REO (wt.%)		
	ZnO	Bi_2O_3	Sb_2O_3	MnO_2	Co_3O_4	Cr_2O_3	NiO	B_2O_3	MgO	Al_2O_3	Pr_6O_{11} ; Y_2O_3	La_2O_3 ; Ce_2O_3	Pr_6O_{11}
SC	95.7	1.0	1.0	0.5	0.5	0.5	0.5	0.1	0.1	0.1	0.01; 0.02; 0.1; 0.25; 0.5		
CR	94.2	1.0	2.5	0.5	0.5	0.5	0.5	0.1	0.1	0.1			

where V_{sb} and V_{sa} are the threshold voltages, respectively, before and after degradation by two short duration shocks of 5 kA,

- energy absorption capability calculated with the approximation:

$$A (J) = 20.8V_m I_m \times 10^{-6} \quad (5)$$

where V_m and I_m are, respectively, the maxima visualized by the oscilloscope for a short duration shock of about 4/10 μ s with amplitudes of 0–65 kA. This value of A divided by the volume of the sample gives the value of A in J/cm^3 .

3. Results and discussions

3.1. Standard composition REO doping

The addition of REO to the ZnO-based varistors composition leads to electrical properties changes. In order to investigate this evolution further we have varied the amounts and the nature of the REO components and examined the electrical properties. The results are gathered in Table 2 and represented in Fig. 1.

The correlation between the composition and electrical characteristics lead to the following remarks:

- there are practically no differences between the effects of the various REO;
- there is not significant increase of the threshold voltage. An increase of 30% maximum is observed with the 0.1 wt.% of REO addition;

Table 2
Electric properties of the REO doped varistors

REO (wt.%)	Threshold voltage, V_s (V/mm)	Degradation, D (%)	Energy absorption capability, A (J/cm^3)
Pr₆O₁₁			
0.01	210	10	110
0.05	230	12.5	111
0.1	250	15	112
0.25	265	17	112
0.5	280	18	113
Y₂O₃			
0.01	217	7	110
0.05	231	8.5	105
0.1	245	10	100
0.25	247	15	102
0.5	248	20	105
La₂O₃			
0.01	220	5	110
0.05	245	6	119
0.1	270	7	127
0.25	280	11	121
0.5	290	15	115
Ce₂O₃			
0.01	230	5	112
0.05	240	12	116
0.1	250	18	119
0.25	270	20	115
0.5	290	22	110

- degradation is accentuated with REO addition. Between 0.01 and 0.1 wt.% of REO, D is somewhat acceptable (around 10%), but beyond 0.1 wt.% it becomes strong, up to 20%;
- energy absorption capability remains good (more than 100 J/cm^3). It is practically constant whatever the REO percentage.

The analysis of the microstructure of the ceramic samples by SEM shows that the REO are mainly located at the triple joints where the pyrochlore phases ($Zn_2Bi_3Sb_3O_{14}$) are usually detected [19]. Moreover those areas appear to be larger with REO compositions suggesting extra-pyrochlore phase formation.

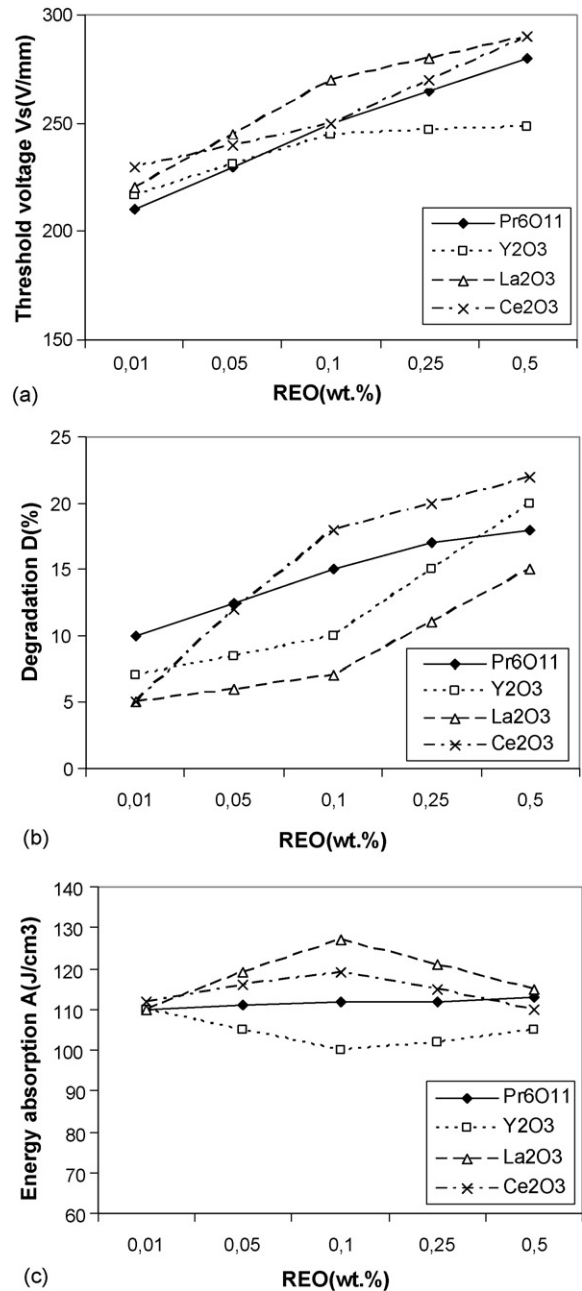


Fig. 1. Varistor electrical characteristics evolution compared to concentration of various REO: (a) threshold voltage (V_s), (b) degradation and (c) energy absorption capability (A).

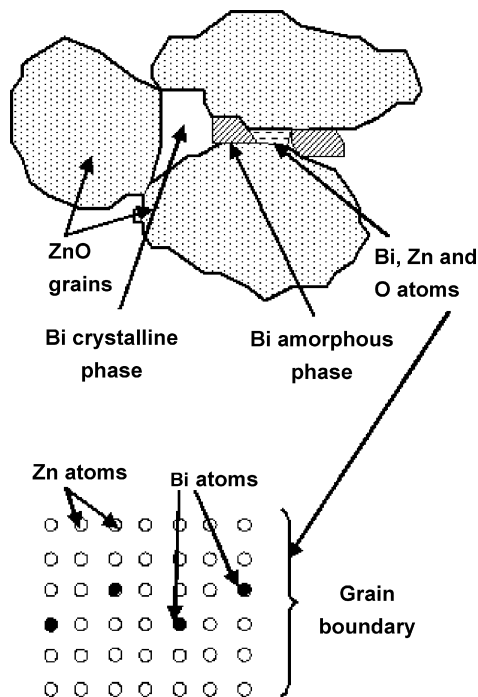


Fig. 2. Model of bismuth continuous phases at the grain boundaries proposed by Kobayashi et al.

Kobayashi et al. [19] showed that there are three Bi-rich phases which form a continuous phase between the grains. The crystalline bismuth phase is at the triple joints. Its width is about 300–500 Å. It changes when it progresses towards the grain boundary in an amorphous phase, and its width decreases to fall from 100 to 200 Å.

And then on the contact surface between two grains, there are only bismuth atoms which alternate with zinc or oxygen atoms. It is the potential Schottky barrier formation cause (Fig. 2).

The spinel ($Zn_7Sb_2O_{12}$) grains are typically 2–4 μm in diameter and form well-faceted octahedral crystals [5]. It may change with the progress to the grain boundary in first an amorphous phase sandwiched between crystalline phases [19] and then only amorphous phase of a width about 100 Å, up to 20 Å. Eventually, there may be only segregated bismuth atoms which alternate with oxygen or zinc atoms [20]. The Bi layer can no longer be regarded as a phase.

It appears that the formation of the Schottky potential barriers, which is at the origin of the varistor effect, is mainly due to these alternate layers [16]: very thin amorphous layer and bismuth atomic layer. However, varistors are multi-junction device with many junctions in parallel and series [5]. The more junctions that are connected in series, the higher the voltage rating and as more junctions are connected in parallel, the higher the current rating. In other words, the threshold voltage is determined by thickness and current discharge so the energy absorption capability is determined by electrode area. When the varistor is operating, the grain boundaries become conductive. They dissipate a part of the electrical energy contained in transient voltage pulses as heat. The grain boundaries define a three-dimensional current path throughout the bulk ceramic. The more conducting path through the atoms layer defines a

conduction section which only it actually controls the energy absorption capability. This explains the fact that the increase in the threshold voltage, therefore the reduction in the ZnO grains size by spinel phase formation at grain boundaries, is always followed by a reduction in the energy absorption capability, since with the reduction in the grains size there is a reduction in the conduction section.

Our results suggest that REO act as grain growth retardants while not shrinking the conduction section as observed with antimony oxide [10]. These results lead us to use REO in antimony-rich composition exclusively to avoid the reduction of the energy absorption.

3.2. Antimony-rich composition

Three types of samples were elaborated using CR: S1 indicates the samples elaborated without REO, S2 the samples in which is added 1 wt.% of Pr_6O_{11} and S3 the samples in which is added 1 wt.% of Nd_2O_3 .

X-ray diffraction (XRD) analysis of the samples S1, S2 and S3 allows phases identification in ceramics (Fig. 3): a ZnO grain phase, a Bi-rich phase and a spinel phase. From the pyrochlore phase there are some XRD peaks for S1, and it is the same for S2 where there are some traces, but for S3 it could not be detected. For the spinel phase, there are XRD peaks of S1 considerably larger than for S2 and S3.

The S1, S2 and S3 photomicrostructures (Fig. 4) show their compositions and distributions, as well as the morphology of the ZnO grains and spinels.

The existing phases are confirmed by both SEM/SRD and XRD analysis. Moreover, it shows that with REO, the spinel grains are smaller and spread over the ceramic bulk. In addition, a new phase which contains REO is observed: $Bi_{1.8}Zn_{2.9}Sb_{2.2}Pr_{0.4}O_x$ for S2 and $Bi_{1.0}Zn_{4.2}Sb_{1.8}Nd_{1.0}O_x$ for S3 and it is located in fine grains distributed along the grain boundaries. From results summarized in Table 3, it is observed that: the S2 spinel grains size is smaller than that of S3; the S2 ZnO grains average size is smaller and more homogeneous than that of S3 because the small spinel grains block more indeed the ZnO grains growth. Thus, the latter become larger and less homogeneous.

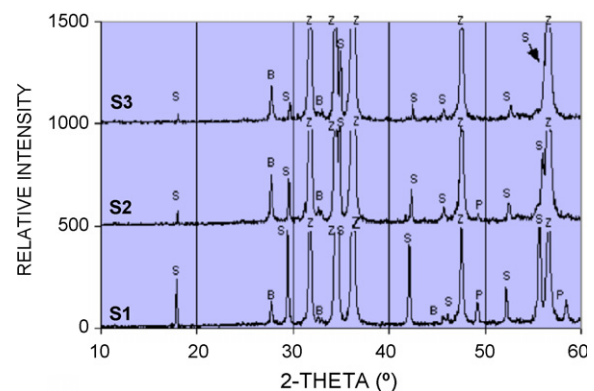


Fig. 3. XRD diagrams (CR): without Pr_6O_{11} (S1), with Pr_6O_{11} (S2) and with Nd_2O_3 (S3). (Z: ZnO phase, S: spinel phase, B: bismuth-rich phase, P: pyrochlore phase).

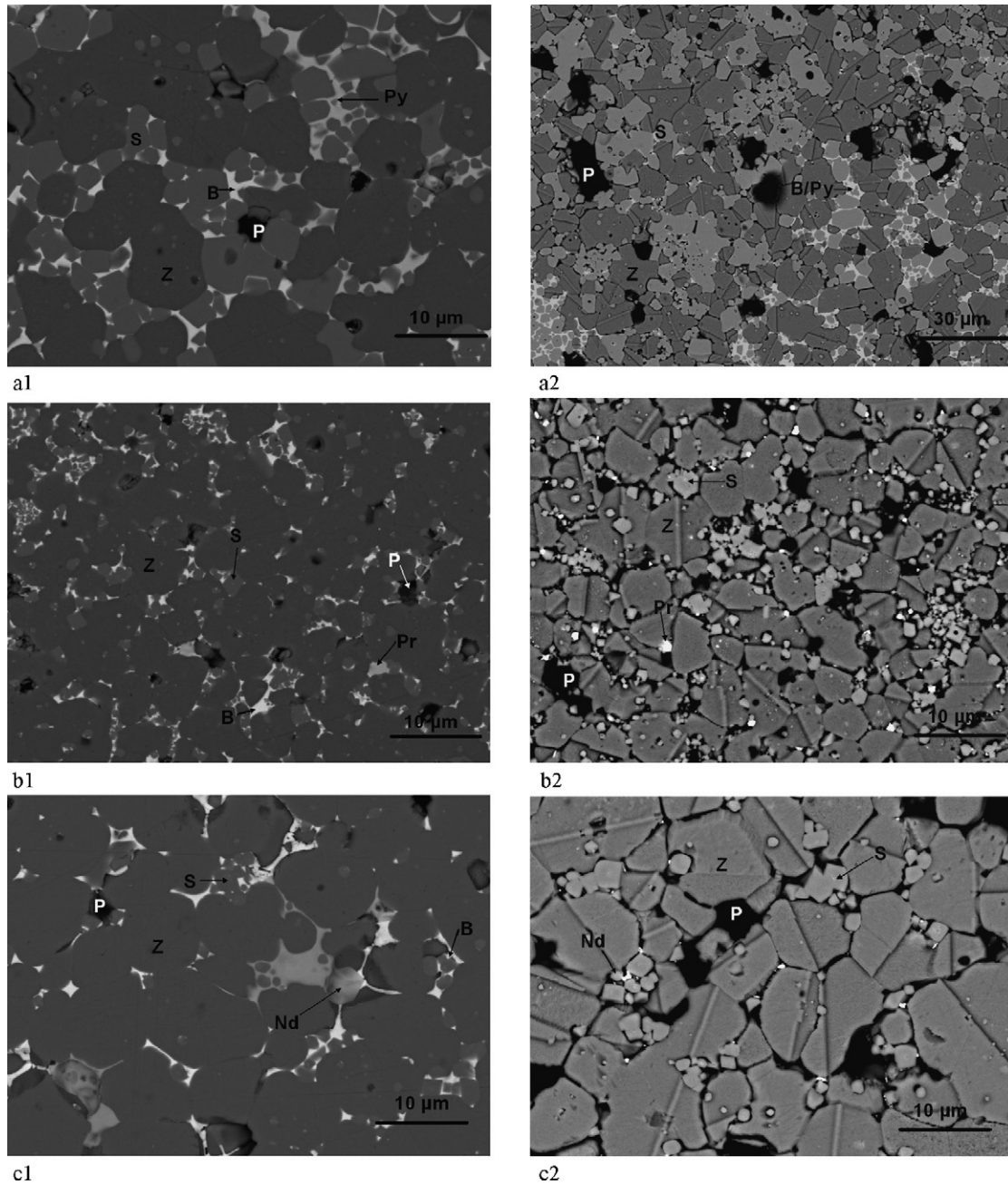


Fig. 4. Microstructures of samples, composition and distribution of the phases: SEM (a1, b1, c1)/SRD (a2, b2, c2). a1 and a2 without REO; b1 and b2 with Pr_6O_{11} ; c1 and c2 with Nd_2O_3 . Z: ZnO phase; S: spinel; B: bismuth-rich phase; Py: pyrochlore; Pr: pyrochlore contains praseodymium; Nd: pyrochlore contains neodymium; P: pores.

In short, the REO influence on the samples microstructure is very significant. Both sizes of the ZnO grains and spinel phases decrease. Compared to the case without REO, the main REO effect is to return the microstructure of more homogeneous varistor, due to spinel phases and pyrochlore (with Pr and with Nd) finer formation which distribute everywhere in the ZnO grains junction length.

The results might be explained from the microstructure formation. During heating several new phases are formed, from the mixed and pressed single oxides raw materials, depending on the parameters of the process, such as heating rate and chemical composition. Among them spinel-type phase, ($\text{Zn}_7\text{Sb}_2\text{O}_{12}$) and a pyrochlore-type phase ($\text{Zn}_2\text{Bi}_3\text{Sb}_3\text{O}_{14}$) play a specific role

during the sintering [21]. The former one acts as a grain growth moderator for ZnO by anchoring the boundaries during sintering. The second one is unstable and decomposes during the sintering.

During the first stage of sintering heterogeneous reactions from the powder particles lead to spinel phases [22,23]:



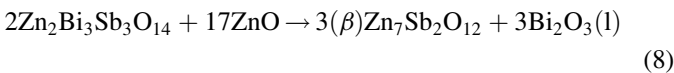
In a second stage a low melting point eutectic between ZnO, Bi_2O_3 and Sb_2O_3 is formed above about 700 °C and a non-negligible amount of additives, REO included, dissolve in this

Table 3
Average grain sizes D , with variance σ , of the ZnO grains, spinels and pores, of the samples: S1 (without REO), S2 (with Pr_6O_{11}) and S3 (with Nd_2O_3)

Sample	ZnO		Spinel		Pore	
	D (μm)	σ	D (μm)	σ	D (μm)	σ
S1	6.7	2.9	2.1	1.5	6.3	5.9
S2	4.7	1.9	0.7	0.4	2.1	0.9
S3	8.7	3.6	1.3	0.7	3.6	2.0

melt. The third stage, liquid phase densification at the sintering temperature is the step where the main ZnO grain growth occurs.

At this temperature the ZnO grains are still small but tend to grow with the temperature despite the presence of spinel phases which hinder ion transfer. As a result the grain growth is limited by pinning migrating ZnO grain boundaries. Another reaction leads to the pyrochlore phase ($\text{Zn}_2\text{Bi}_3\text{Sb}_3\text{O}_{14}$) formation which is rather unstable and decomposes during the early stage of sintering by solid-state reaction of ZnO with pyrochlore ($\text{Zn}_2\text{Bi}_3\text{Sb}_3\text{O}_{14}$) according to [21]:



which gets free liquid Bi_2O_3 -rich phase above 950 °C.

During cooling, Bi-rich phase recedes to multigrain junctions. This operation is critical since extra bismuth concentration is rather detrimental to produce good varistor electrical properties [19,20]. The spinel phases, embedded in the liquid, are expelled to the multi-junctions. This creates a microstructure constituted of ZnO grains where the space at multiple-grain junctions and partially surrounding ZnO grains are filled by bismuth rich phase.

REO promotes apparently the pyrochlore phase formation. Furthermore, according to Eq. (8) and in agreement with experimental results presented in Table 3, there is less liquid for material transfer and for spinel growth. In other words, the “pinning action” of the spinel grains depends directly on the pyrochlore formation and decomposition.

The conduction section with the grain boundaries is maintained, from where a conservation of the energy absorption capacity presented in Table 4: 107 J/cm^3 whereas it had fallen to 52 J/cm^3 because of the great quantity of Sb_2O_3 .

From results summarized in Table 4, we elucidate the following significant points:

- *Little change of the threshold voltage*: the rate of increase in threshold voltage between S1 and S2 or S3 is about 8–12%. In

Table 4
Electrical properties of the samples: S1 (without Pr_6O_{11}) and S2 (with Pr_6O_{11})

Sample	Non-linearity coefficient, α	Threshold voltage, V_s (V/mm)	Energy absorption capability, A (J/cm^3)
S1	42	280	52
S2	40	312	107
S3	52	302	112

the S2 case, the average size of ZnO grains decreases by the order of 30%. That makes it possible its threshold voltage to increase approximately by 11%. In this case, therefore, it is possible that the effect of the ZnO grains' size plays a more significant role than that of the voltage barrier height. On the contrary, in the S3 case, the average size of ZnO grains will increase in order of 23%, while its threshold voltage increases by 7%. This suggests that the dominating role is played by the voltage barrier height.

- *High increase in the energy absorption capability A*: for S1 A is equal to 52 J/cm^3 , but with Pr_6O_{11} and Nd_2O_3 addition, A growth with a value twice larger for S2 and also for S3. The A low value for S1 is allotted to the great quantity of spinel grains clusters which exist in this sample. The spinel phase has in the effect, a great resistivity [17]. Therefore, the ZnO–spinel junction does not contribute to the non-linear effect. Moreover, in S1, the spinels form in particular clusters along the ZnO grain boundaries. Such an isolated spinels chain reduces the current flow by tightening the effective conduction section, from where a local increase in temperature and a reduction in energy absorption capability.

The morphology of ceramics is strongly modified by the presence of a small quantity of REO. Insulating spinel clusters are transformed into individual spinel grains which are distributed alternatively with pyrochlore phases Pr or Nd to the place of the triple joints of ZnO grains. There remain only ZnO grains and grain boundaries in the conduction chain between electrodes. It results that the energy absorption capability increases.

In addition, one finds that a small quantity of pyrochlore for S2 and S3 is explained by Co excess, Mn, Ni, . . . , atoms which enter the ZnO grains and increase their conductivity, thus bringing the saturation area towards the high currents.

4. Conclusions

The rare earth oxides increase the threshold voltage, but not in a significant way, only of one about thirty percent. They also make it possible to obtain a considerable increase in the capacity for absorption in energy, thanks to the varistor microstructure morphology transformation. The rare earth oxide makes it also possible the ZnO grains to preserve the effective conduction section. A composition rich in antimony oxide will have with rare earth oxide a double effect. On the one hand, a high threshold voltage (300 V/mm) ensured by antimony oxide, and on the other hand, a good capacity for absorption in energy (100 J/cm^3) ensured by the REO. Spinel clusters have been found to give formation to barriers against electrical conduction.

Acknowledgment

The authors thank Mr. S. Bernik, senior research associate in Josef Stefan Institute, Ljubljana, Slovenia, for his active collaboration in the realization of the microstructural analyses.

References

- [1] M. Matsuoka, Nonohmic properties of zinc oxide ceramics, *Jpn. J. Appl. Phys.* 10 (6) (1971) 736–746.
- [2] K. Eda, Zinc oxide varistors, *IEEE Electrical Insulation Mag.* 5 (6) (1989) 28–41.
- [3] E. Olsson, L.K.L. Falk, G.L. Dunlop, R. Osterlund, The microstructure of the ZnO varistor, *J. Mater. Sci.* 20 (1985) 4091–4098.
- [4] T.K. Gupta, Application of zinc oxide varistors, *J. Am. Ceram. Soc.* 73 (7) (1990) 1817–1840.
- [5] L.M. Levinson, H.R. Philipp, Zinc oxide varistors—a review, *Ceram. Bull.* 65 (4) (1986) 639–646.
- [6] M. Inada, Crystal phases of nonohmic zinc oxide ceramics, *Jpn. J. Appl. Phys.* 17 (3) (1978) 1–10.
- [7] A. Bui, H.T. Nguyễn, A. Loubière, High-field ZnO-based varistors, *J. Phys. D: Appl. Phys.* 28 (1995) 774–782.
- [8] T. Takemura, M. Kobayashi, Y. Takada, K. Sato, Effects of antimony oxide on the characteristics of ZnO varistors, *J. Am. Ceram. Soc.* 70 (4) (1987) 237–241.
- [9] K. Jinho, T. Kimura, T. Yamaguchi, Sintering of zinc oxides doped with antimony oxide and bismuth oxide, *J. Am. Ceram. Soc.* 72 (8) (1989) 1390–1395.
- [10] J. Wong, Microstructure and phase transformation in a highly non-ohmic metal oxide varistor ceramic, *J. Appl. Phys.* 46 (4) (1978) 2407–2411.
- [11] A.B. Alles, V.L. Burdick, The effect of liquid-phase sintering on the properties of Pr₆O₁₁-based ZnO varistors, *J. Appl. Phys.* 70 (11) (1991) 6883–6890.
- [12] A.B. Alles, R. Puskas, G. Callahan, V.L. Burdick, Compositional effect on the liquid-phase sintering of praseodymium oxide-based zinc oxide varistors, *J. Am. Ceram. Soc.* 76 (8) (1993) 2098–2102.
- [13] S.Y. Chun, K. Shinozaki, N. Mizutani, Formation of varistor characteristics by the grain-boundaries penetration of ZnO–PrO_x liquid into ZnO ceramics, *J. Am. Ceram. Soc.* 82 (1999) 3065–3068.
- [14] Y.-S. Lee, K.-S. Liao, T.-Y. Tseng, Microstructure and crystal phases of praseodymium in zinc oxides varistor ceramics, *J. Am. Ceram. Soc.* 79 (1996) 2379–2384.
- [15] C.-W. Nahm, C.-H. Park, H.-S. Yoon, Microstructure and varistor properties of ZnO–Pr₆O₁₁–CoO–Nd₂O₃ based ceramics, *J. Mater. Sci. Lett.* 19 (2000) 271–274.
- [16] K. Mukae, K. Tsuda, I. Nagasawa, Non-ohmic properties of ZnO-rare earth metal oxide-Co₃O₄ ceramics, *Jpn. J. Appl. Phys.* 16 (8) (1977) 1361–1368.
- [17] K. Mukae, Zinc oxide varistors with praseodymium oxide, *Ceram. Bull.* 66 (9) (1987) 1329–1331.
- [18] N. Wakiya, S.Y. Chun, C.H. Lee, O. Saakurai, K. Shinozaki, N. Mizutani, Effect of liquid phase and vaporization on the formation of microstructure of Pr doped ZnO varistor, *J. Electroceram.* 4 (1) (1999) 15–23.
- [19] K.I. Kobayashi, O. Wada, M. Kobayashi, Y. Takada, Continuous existence of bismuth at grain boundaries of zinc oxide varistor without intergranular phase, *J. Am. Ceram. Soc.* 81 (8) (1998) 2071–2076.
- [20] T. Asokan, Effect of dopants' distribution on the non-linear properties of a ZnO based resistor, *Br. Ceram. Trans. J.* (80) (1987) 187–189.
- [21] M. Inada, Formation mechanism of nonohmic zinc oxide ceramics, *Jpn. J. Appl. Phys.* 19 (3) (1980) 409–419.
- [22] M. Inada, Effect of heat-treatment on crystal phases, microstructure and electrical properties of nonohmic zinc oxide ceramics, *Jpn. J. Appl. Phys.* 18 (8) (1979) 1439–1446.
- [23] J. Kim, T. Kimura, T. Yamaguchi, Microstructure development in Sb₂O₃-doped ZnO, *J. Mater. Sci.* 24 (7) (1989) 2581–2586.